

Two-photon processes in faint biphoton fields

Dmitry V. Strekalov, Matthew C. Stowe, Maria V. Chekhova*
and Jonathan P. Dowling.

Quantum Computing Technologies Group, Sect. 367,
Jet Propulsion Laboratory, California Institute of Technology,
MS 300-123, 4800 Oak Grove Drive, Pasadena, CA 91109.

Dmitry.V.Strekalov@jpl.nasa.gov

*Moscow State University,
Moscow, Russia

February 25, 2019

Abstract

The goal of this research is to determine and study a physical system that will enable a fast and intrinsically two-photon detector, which would be of interest for quantum information and metrology applications. We consider two types of two-photon processes that can be observed using a very faint, but quantum-correlated *biphoton* field. These are optical up-conversion and an external photoelectric effect. We estimate the correlation enhancement factor for the biphoton light compared to coherent light, report and discuss the preliminary experimental results.

1 Introduction

The term “biphoton” has been suggested by D.N. Klyshko [1] for describing systems of entangled photon pairs, such as those produced in the Spontaneous Parametric Down Conversion (SPDC) of light¹. In this process, a pump photon is coherently converted into a pair of entangled photons in a $\chi^{(2)}$ medium [2], while the phase and spectral properties of the pump are transferred to the biphoton [3, 4]. This phase then can be recovered by a two-photon correlation measurement. In this context, describing this system as “two photons” is not complete and even may be misleading as it tends to omit the quantum correlation properties of the photon pair [5, 6]; so the term “biphoton” proves to be very useful.

¹In acknowledgment of D. N. Klyshko’s founding role in studies of parametric processes in optics, SPDC is sometimes referred to as “Klyshko radiation”.

A pair of entangled particles that are space-like separated is an excellent system for testing the concepts of physical *locality* and *reality* [7]. Therefore it is not surprising that SPDC has received great attention as an entanglement source for Bell inequalities tests. The whole variety of such tests can be generally described as nonlocal biphoton interference experiments. As a further development, experiments involving higher-order interference have been carried out, such as the Greenberger-Horne-Zeilinger theorem test [8] and quantum teleportation [9, 10].

Besides purely a fundamental interest, study of the biphoton light has inspired development of new information and measurement technologies, such as quantum cryptography [11], sub-shot noise optical phase measurements [12–14], quantum clock synchronization [15, 16], and others. Most recently, the possibility of sub-diffraction-limited imaging [14] and lithography [17–21] has been discussed. There is a clear shift of the research in biphoton optics towards practical applications. It is also clear that the difficulties on the path to such applications are quite severe and have one common root, which is the detection problem.

Consider quantum cryptography, which is generally believed to be the most mature of quantum optical technologies. It has been shown [22] that the main limitation blocking its practical implementation is the single-photon detection rate. It is not possible, with the state-of-art single-photon detectors, to achieve the detection rate that would make useful wideband quantum crypto-communication channels [22]. Similarly, quantum optical interferometers are theoretically capable of being noise-limited at the fundamental (Heisenberg) level $1/\sqrt{\langle n \rangle}$, while the classical shot-noise limit is $1/\sqrt{\langle n \rangle}$ ($\langle n \rangle$ being the mean number of photons per measurement). Therefore the quantum measurement of the phase has advantage over the classical one only when $\langle n \rangle$ is large. But for a large photon flux, any coincidence detection technique will fail because of the finite dead time of photon counting detectors and coincidence circuit time-windows. Thus again, the detection rate of photon pairs is the limiting factor here. The situation gets even more complicated for quantum lithography, where the two-photon detectors are molecules in the resists that are small and distributed in the media. Here one has to worry not only about the detection rate, or fast two-photon sensitivity, but also about the transverse correlation properties of the biphoton light.

Therefore the search for fast two-photon processes that could enable a true two-photon detector (as opposed to an electronic coincidence circuit), that could be used for study of strong biphoton fields, becomes one of the most important questions of the applied quantum optics. So far, no two-photon processes induced by the biphoton field have been demonstrated. On the other hand, two-photon processes in strong classical fields, such as pulsed laser fields, have been studied quite extensively.

The goal of our research is to analyze the possibility of direct two-photon detection of the biphoton field and to determine the physical system which is most suitable for this purpose. In the following sections we will demonstrate the advantage of biphoton light over coherent light for driving two-photon processes. This advantage will be shown considerable enough to make up for extremely low power of the biphoton sources such as SPDC. Then,

we will discuss two types of processes that could serve for direct two-photon detection: optical up conversion and the photo-electric effect.

2 Biphoton field and coherent field

We will use a conventional concept of a photon detection event [23], which takes place with a probability $P^{(1)}$ proportional to a constant η (the *quantum efficiency* of the detector) and to the probability to have one photon in the mode volume, which is equal to coherence volume V_c , scaled to the *detection volume*. In case of free-space propagation, V_c is given by the product of coherence length and coherence cross section of the light beam. The detection volume is defined as the detector's cross section S_d multiplied by the observation time t and by the speed of light c . E.g., for ordinary coherent laser light with Poissonian distribution of photons,

$$P^{(1)} = \eta^{(1)} \langle n \rangle \frac{S_d ct}{V_c} e^{-\langle n \rangle} \propto \eta^{(1)} I S_d ct, \quad (1)$$

where I is the intensity and $\langle n \rangle = \langle a^\dagger a \rangle$ is the mean number of photons per mode. We assume $\langle n \rangle \ll 1$, which justifies neglecting the exponent in Eq. (1). Likewise, the probability to detect a photon *pair* in a coherently populated mode is:

$$P^{(2)} = \eta^{(2)} \frac{\langle n \rangle^2}{2} \frac{S_d ct}{V_c} e^{-\langle n \rangle} \propto \eta^{(2)} I^2 S_d ct. \quad (2)$$

The quantum efficiency η in (1) and (2) are labeled with the superscript indicating the single-photon and two-photon types of detection.

In contrast with uncorrelated coherent light, the biphoton light can be viewed as consisting of correlated photon pairs. One can introduce the correlation volume V_{corr} of the paired photons as a product of the longitudinal two-photon correlation length and the transverse two-photon correlation cross-section. An example of how these parameters are defined and treated will be given in the next section. It has been pointed out [1] that if the two-photon correlation volume is significantly smaller than the detection volume, $V_{corr} < S_d ct$, the photon pairs detection probability (2) becomes linear with respect to the light intensity [24], similarly to (1):

$$P^{(2)} = \eta^{(2)} \frac{\langle n \rangle}{2} \frac{S_d ct}{V_c} e^{-\langle n \rangle/2} \propto \eta^{(2)} I S_d ct. \quad (3)$$

Indeed, equation (3) represents the probability to detect a photon pair, when the pairs themselves are randomly distributed. The random distribution of pairs is specific for the SPDC process [25]. This fact is important for the argument concerning the use of SPDC as an allegedly more secure photon source for quantum cryptography. Both the photon distribution in an attenuated laser pulse (coherent state) and the pairs distribution in SPDC have Poissonian statistics and hence are equally likely to compromise security by accidental duplication of the encoded states.

Comparing the two-photon detection probabilities for coherent light, Eq. (2), and for biphoton light, Eq. (3), one notices that the latter is greater than the former by a factor of $\langle n \rangle^{-1}$ [1]. Let us estimate this factor for the case of SPDC. The biphoton enhancement factor can be expressed in terms of brightness as [25]

$$\frac{1}{\langle n \rangle} \equiv \frac{S_0}{S}, \quad (4)$$

where the brightness S is

$$S \equiv \frac{I}{\Delta\omega\Delta\Omega}, \quad (5)$$

$\Delta\omega$ is the observed spectral range of frequencies, $\Delta\Omega$ is the solid angle and the *vacuum brightness* S_0 is

$$S_0 \equiv \frac{\hbar c}{\lambda^3}. \quad (6)$$

We consider a Type-I BBO crystal near collinear degenerate phase matching with the central wavelength $\lambda_0 = 702$ nm, in which case $S_0 \approx 10^{-11}$ J/cm². The *independent* variations of ω and Ω can be estimated from the tuning curves and spectral linewidth of SPDC light (see Fig.1): $\Delta\omega \approx 10^{13}$ s⁻¹, $\Delta\Omega \approx 0.2$ sr. The typical light power we get from a 5 mm - long Type-I BBO crystal is 50 nW. This SPDC light is generated by the pump beam that is approximately 200 microns in diameter. Combining these numbers we get $S \approx 10^{-16}$ J/cm², which yields the enhancement factor $\langle n \rangle^{-1} \approx 10^5$.

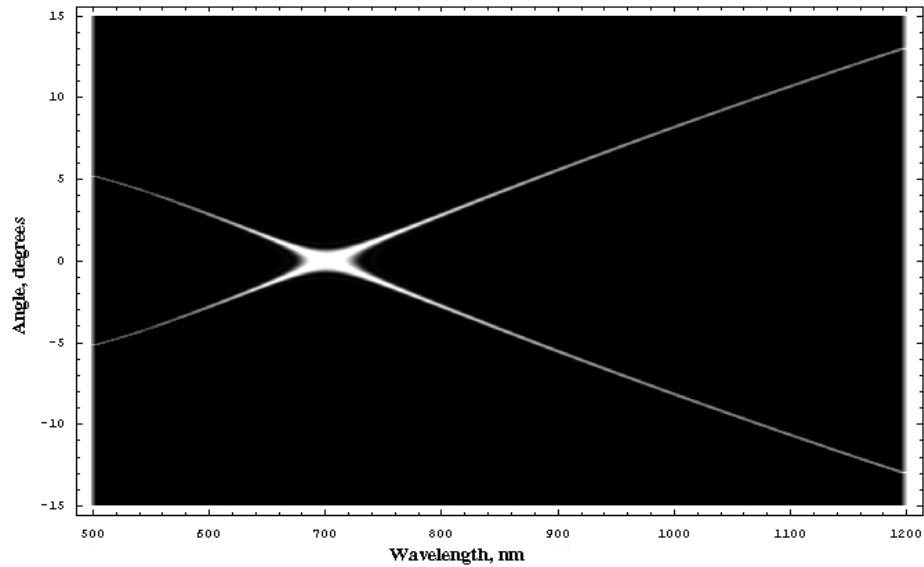


Figure 1: The tuning curves and spectral linewidth for a 5 mm Type-I collinear degenerate BBO.

3 Up-conversion of biphoton field

One possible method for two-photon detection is up conversion. This is a nonlinear optical process that is the time-reverse of SPDC. The frequency-degenerate case of this process, second harmonic generation, is routinely used in autocorrelators to measure the duration of very strong and short optical pulses. The large value of the enhancement factor $\langle n \rangle^{-1}$ for the biphoton light suggests that the optical up conversion can be seen from such light, despite a typically very low efficiency of this process. It should be possible, using a pair of similar nonlinear crystals (the first one for SPDC and the second one for the up conversion) to detect the up-converted UV photons emitted from the second crystal. An interesting feature of this system is that the two-photon detection and correlation volumes are equal. This makes our system simpler for analysis than most of other two-photo detection schemes where the relation between these two volumes is not obvious, and the key assumption $V_{corr} < S_d ct$ may fail. The photon pairs emitted from a localized source at various angles can be all brought together with a diffraction-limited error and while preserving the phase-matching conditions (that are equivalent for SPDC and for the up conversion) by an imaging system with a unity magnification. In Fig.2, such a system is represented by a lens placed between the two nonlinear crystals at the distance $2f$ from each.

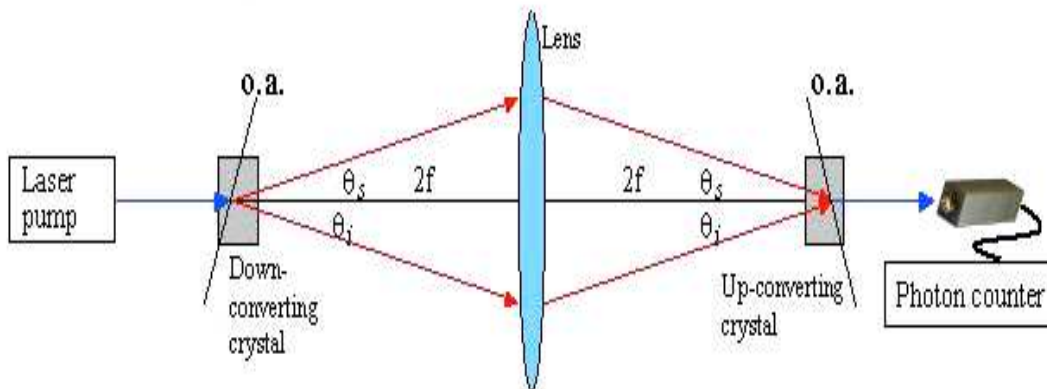


Figure 2: A conceptual drawing of the experiment on up conversion of biphoton light. o.a. stands for the optical axes of the nonlinear crystals.

A rough estimate of the expected detection rate of the up-converted UV photons can be done based on the above-found biphoton enhancement factor and on the experimental observation that a 1 Watt CW pump focused down to about 200 microns on a BBO crystal similar to the one we use for up-conversion produces approximately $10 \mu\text{W}$ of the second harmonic. Scaling this number quadratically to a 50 nW pump power, we get 2.5×10^{-20} W of the up-converted light, or about 0.3 photons per second. To take the biphoton nature of our “pump” into account, we multiply this number by the enhancement factor, arriving at some thirty thousand photons per second. Even with a 1% - efficient photomultiplier tube, this should produce an easily detectable signal of some 300 counts per second. This number

gets significantly lower if a more careful evaluation is carried out, and various mechanisms of the phase mismatch are taken into account. To perform such an evaluation we need to understand the transverse correlation properties of a biphoton.

While the longitudinal (temporal) correlation in the biphoton field has been extensively studied in both theory and experiment, starting from the pioneering works [26, 27], the studies of its transverse correlation are few. A very broad theoretical description is given in [28]; theoretical analysis along with experimental data is also presented in [3]; study of biphoton propagation through generic imaging systems is reported in [29, 30]. Summarizing the analysis from [3], we write the quantum state of a biphoton emitted in a monochromatically pumped SPDC process as

$$|\Psi\rangle = \int F(\vec{k}_s, \vec{k}_i) |1\rangle_{\vec{k}_s} |1\rangle_{\vec{k}_i} d\vec{k}_s d\vec{k}_i, \quad (7)$$

where the delta-like two-photon amplitude $F(\vec{k}_s, \vec{k}_i)$ which entangles the *signal* SPDC mode labeled by its wave vector \vec{k}_s with the *idler* mode \vec{k}_i breaks up into a product of its longitudinal and transverse parts:

$$F(\vec{k}_s, \vec{k}_i) = F_x(\Delta\omega, \Delta\theta_s, \Delta\theta_i) F_z(\Delta\omega, \Delta\theta_s, \Delta\theta_i). \quad (8)$$

In Eq. (8), the arguments of the two-photon amplitude F , representing the wave vectors and frequencies of the signal and idler photons, are first replaced by the variations of these values from their central values that satisfy the phase matching conditions

$$\begin{aligned} \omega_p &= \omega_{s0}(\vec{k}_{s0}) + \omega_{i0}(\vec{k}_{i0}), \\ \vec{k}_p &= \vec{k}_{s0} + \vec{k}_{i0}, \end{aligned} \quad (9)$$

so that

$$\begin{aligned} \Delta\omega &\equiv \omega_s(\vec{k}_s) - \omega_{s0}(\vec{k}_{s0}) = \omega_{i0}(\vec{k}_{i0}) - \omega_i(\vec{k}_i), \\ \Delta\vec{k}_s &\equiv \vec{k}_s - \vec{k}_{s0}, \\ \Delta\vec{k}_i &\equiv \vec{k}_i - \vec{k}_{i0}. \end{aligned} \quad (10)$$

Then, the longitudinal (z) and transverse (x) components of the phase mismatch $\Delta\vec{k}_s + \Delta\vec{k}_i$ are expressed via $\Delta\omega$ and the variations of the angles $\Delta\theta_{s,i}$ to result into the expressions for the F_x and F_z in Eq. (8).

The physical meaning and the use of the two-photon amplitude (8) is quite transparent. One can set $\Delta\theta_{s,i} = 0$ and study only the temporal, or longitudinal, correlation of the biphoton. This is often done since such an approximation describes the most usual type of experiments with SPDC, when the signal and idler modes are selected by a set of narrow pinholes. On the other hand, one could collect the biphoton light from a broad range of angles, but through a pair of very narrow band-pass optical filters. This case corresponds to the limit $\Delta\omega = 0$ which gives the angular, or transverse, part of the biphoton amplitude, which we need to find.

As it has been shown in Ref. [3], F_x reflects the properties of the pump angular spectrum and the transverse inhomogeneities of the crystal; it has a Gaussian shape for a Gaussian shaped pump. F_z depends on the polarization and wavelength dispersion properties of the nonlinear crystal. The analysis for a monochromatic Gaussian pump of the diameter a and for a Type-I crystal of the length l yields simple expressions for F_x and F_z as functions of the internal angles $\theta^{(in)}$. Assuming $\Delta\omega = 0$ we have

$$\begin{aligned} F_x &= \exp \left\{ -\frac{(2\pi a)^2}{4} \left(\frac{n(\lambda_s)}{\lambda_s} \cos[\theta^{(in)}(\lambda_s)] \Delta\theta_s^{(in)} - \frac{n(\lambda_i)}{\lambda_i} \cos[\theta^{(in)}(\lambda_i)] \Delta\theta_i^{(in)} \right)^2 \right\}, \\ F_z &= \text{sinc} \left\{ -\frac{2\pi l}{2} \left(\frac{n(\lambda_s)}{\lambda_s} \sin[\theta^{(in)}(\lambda_s)] \Delta\theta_s^{(in)} + \frac{n(\lambda_i)}{\lambda_i} \sin[\theta^{(in)}(\lambda_i)] \Delta\theta_i^{(in)} \right) \right\}. \end{aligned} \quad (11)$$

The wavelengths $\lambda_{s,i}$ correspond to k_{s0} and k_{i0} , and are related by the phase matching conditions (9) to each other and to the angles θ .

It is of interest to point out that F_x is a function of the angular variation differences, while F_z is a function of their sum. Therefore (considering the opposite signs of θ_s and θ_i) F_x defines the range of angles over which both the signal and idler differ from the exact phase-matching directions, while preserving the angle between them. The function F_z defines the range of variation of the angle between the signal and idler. This is similar to factorization of the temporal (longitudinal) part of the biphoton amplitude, which has been shown to break up as a product of functions of the sum and difference of two detection times: $u(t_1 - t_2) \times v(t_1 + t_2)$ [31]. In this case, v takes on the shape of the pump frequency spectrum (and is similar to F_x in the present study) and u depends essentially on the polarization and wavelength dispersion properties of the crystal (and is similar to F_z in the present study).

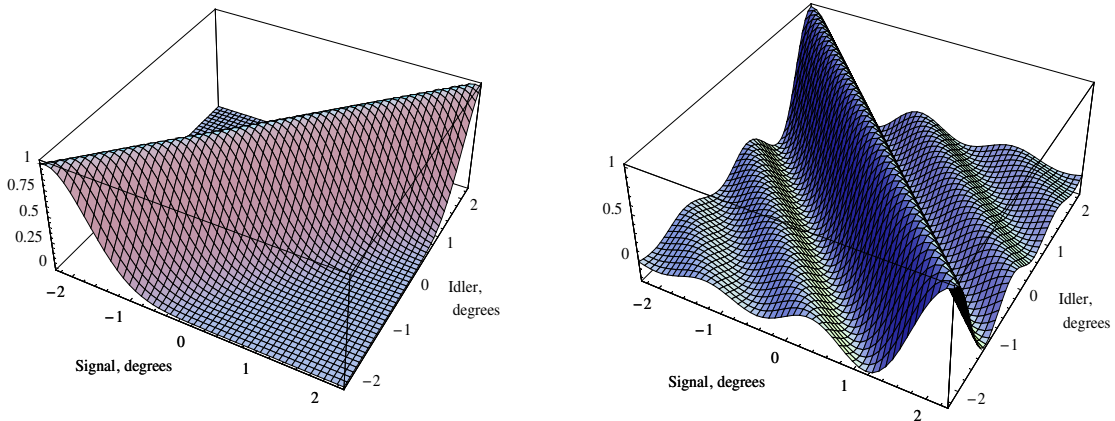


Figure 3: The transverse part of the biphoton amplitude $F_x(0, \Delta\theta_s, \Delta\theta_i)$ (on the left) and $F_z(0, \Delta\theta_s, \Delta\theta_i)$ (on the right). The signal and idler wavelengths are $\lambda_s = 690$ nm, $\lambda_i = 715$ nm.

The internal angles in Eq. (11) may be replaced by the external ones via the Snell's law. The results are shown in Fig.3 for the pair $\lambda_s = 690$ nm, $\lambda_i = 715$ nm. The product

of $F_x(0, \Delta\theta_s, \Delta\theta_i)$ and $F_z(0, \Delta\theta_s, \Delta\theta_i)$ gives $F(0, \Delta\theta_s, \Delta\theta_i)$, whose absolute square can be interpreted as a correlation function of the angular variations $\Delta\theta_s$ and $\Delta\theta_i$. It turns out that the width of F_z strongly depends on the signal and idler wavelength variation from degeneracy (when $\lambda_s = \lambda_i$), getting broader as these wavelengths approach the degenerate values. Three examples of $F^2(0, \Delta\theta_s, \Delta\theta_i)$ for different signal and idler wavelengths are shown in Fig.4, where the middle plot corresponds to the product of functions from Fig.3.

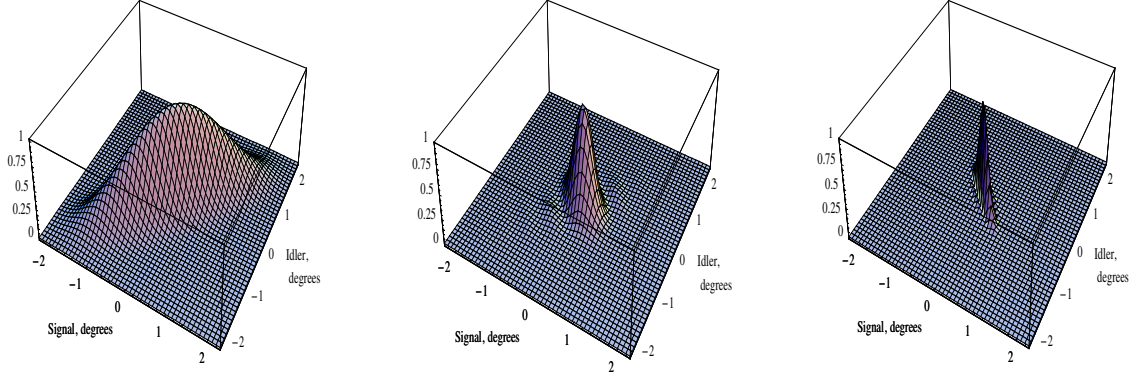


Figure 4: The biphoton transverse correlation functions $F^2(0, \Delta\theta_s, \Delta\theta_i)$. The signal and idler wavelengths are close to degeneracy (on the left); $\lambda_s = 690$ nm, $\lambda_i = 715$ nm (in the center); and $\lambda_s = 650$ nm, $\lambda_i = 754$ nm (on the right).

Understanding of the transverse correlation properties of biphotons allows for a more thorough analysis of the biphoton up-conversion experiment. In particular, it allows us to establish the required degree of precision in alignment of the crystals' optical axes. To do this we substitute the arguments of the correlation function $F^2(0, \Delta\theta_s, \Delta\theta_i)$ with the phase-matching angles variations:

$$\Delta\theta_{s,i} = \frac{\partial\theta_{s,i}}{\partial\alpha}\Delta\alpha, \quad (12)$$

where the derivative is calculated with respect to the angle α between the optical axis and the pump beam. The function obtained from substituting Eq. (12) into $F^2(0, \Delta\theta_s, \Delta\theta_i)$ represents the degree of overlap between the the down- and up-conversion phase matching conditions for crystals whose optical axes are misaligned by $\Delta\alpha$. In the following, we will call it the overlap function. Curiously, this function is practically uniform throughout the entire SPDC spectrum. Fig.5 shows two plots of this function: for degenerate, and for far non-degenerate wavelengths, that look almost as a single line.

From Fig.5 we see that the crystals' optical axes need to be aligned to about 0.2° which is not hard to achieve. A bigger difficulty arises from the finite length of the crystals. Even though the parts of the down-converting crystal displaced from the 1:1 imaging plane still do get imaged onto the up-converting crystal, the signal and idler rays now cross at the angles different from their phase matching angles θ_s, θ_i . These angular errors can be found

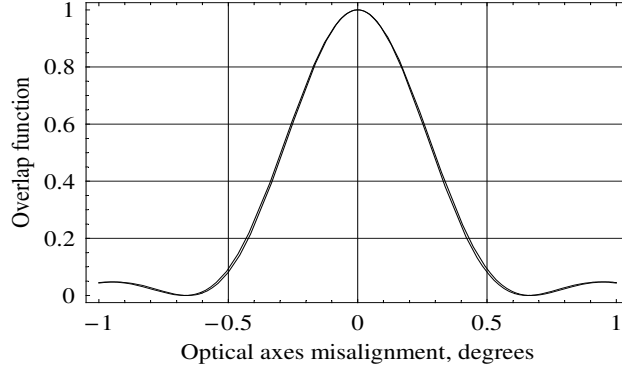


Figure 5: The overlap function vs. misalignment of optical axes of two crystals.

from a simple geometrical considerations as functions of the linear displacement z from the 1:1 imaging plane. Substituting them into $F^2(0, \Delta\theta_s, \Delta\theta_i)$ we find the overlap function as a function of z for different parts of the SPDC spectrum. Integrating this function over z , we find the overall spectral overlap function. From Fig.6 we see that in case of a 5-mm BBO crystal at collinear degenerate phase matching, only a relatively narrow wavelength range can be efficiently up-converted. As a result, the above estimate of 300 counts per second is considerably reduced. These and other difficulties have so far precluded a convincing experimental demonstration of biphoton detection via optical up conversion, however we plan to continue our work in this direction.

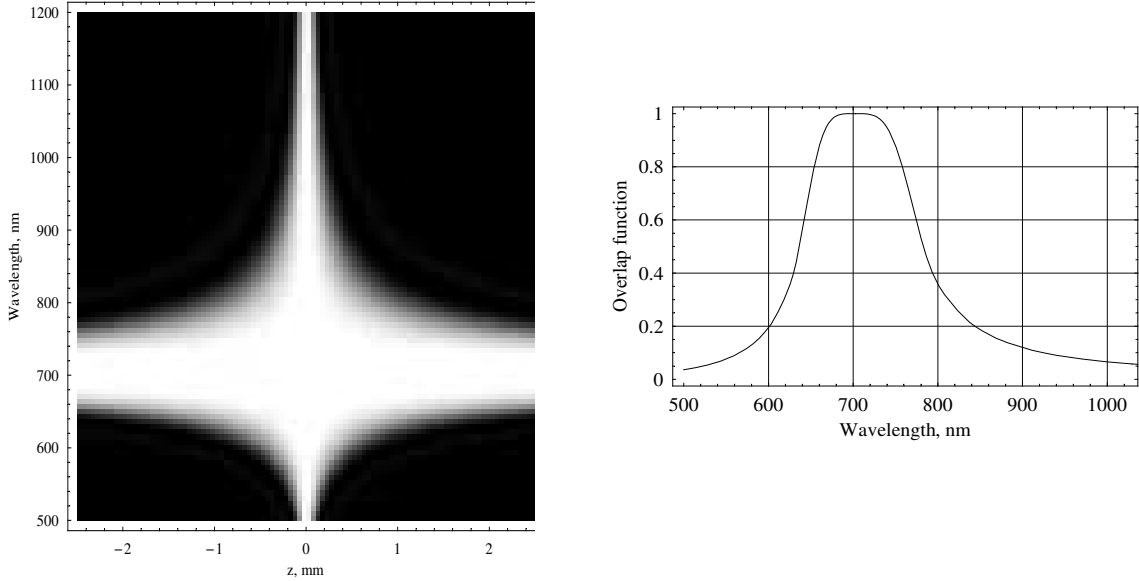


Figure 6: Left: the overlap function vs. the displacement z from the imaging plane and the wavelength. Right: the overlap function for a 5 mm crystal vs. the wavelength.

4 Photo-electric processes in biphoton field

Another system interesting for the study of two-photon processes is a metal or semiconductor surface. If the red threshold of the external photo-electric effect in such a system corresponds to the total energy of the photon pair, one can expect a detectable photo-current corresponding to two-photon processes in the near absence of single-photon photo-current. The advantage of this system over the optical up-conversion is a much larger possible two-photon response cross-section; the disadvantage is that, in practice, such systems are very hard to characterize due to their complexity and a large number of simultaneously occurring physical processes.

Two-photon response of the photo cathodes in photo-multiplier tubes (PMT) has been studied for use in the characterization of temporal properties of ultrafast laser pulses in which the peak intensity is extremely large [32,33]. Two-photon ionization may proceed by a direct two-photon channel via a virtual level, or by an indirect (cascade) process in which the electron may reside in an intermediate state, such as the conduction band or a deep trap, for some period of time. In many cases it may be beneficial to have an intermediate state in single-photon resonance with the light, because it increases the two-photon absorption rate. However, for the observation of two-photon light from SPDC, long-lived intermediate states may lead to a signal from uncorrelated photons, which is undesirable. The purpose of this work is to characterize a potential material for two-photon detection and to develop an understanding of the relevant physics for optimizing a fast two-photon detector. We are interested in observing the two-photon photo-electric effect from biphoton light, initiated by quantum-correlated photon pairs, rather than by absorption of statistically independent pairs of photons. For efficient discrimination between these two competing processes, we need to make sure the longest lifetime of the intermediate states is not much longer than the biphoton correlation time.

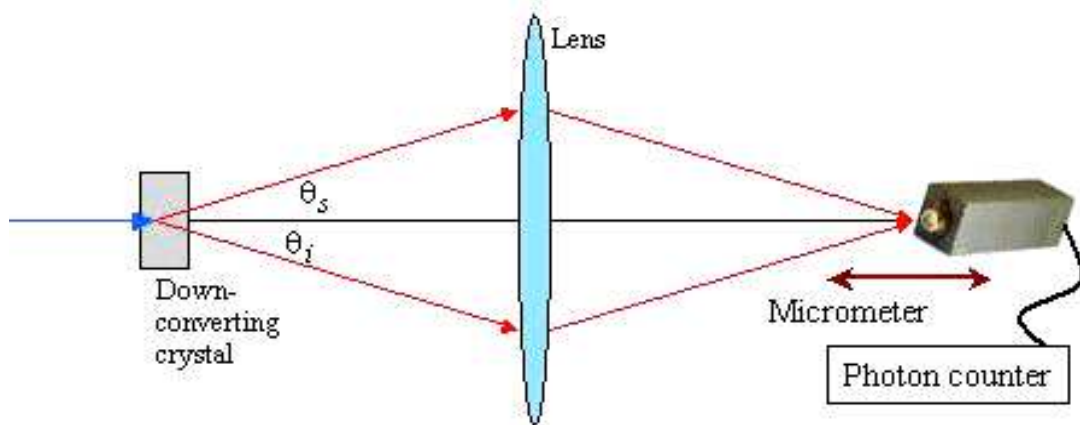


Figure 7: Illustration of the two-photon photo cathode experiment with biphoton light.

In our experiment, we image the biphoton source onto a Cs_2Te photo cathode with diffraction-limited resolution, as illustrated in Fig.7. We use a PerkinElmer MH922P chan-

nel photomultiplier detector in photon counting mode. This CPM has a Cs_2Te cathode which has a bandgap of 3.3 eV and electron affinity of less than 0.5 eV [34]. The peak quantum efficiency, centered at 200 nm, is about 0.1. It falls off to approximately 10^{-3} at our pump wavelength (351.1 nm Argon Ion laser line), and to 10^{-8} at 702 nm, the degenerate signal and idler wavelength. Therefore one might expect to see a two-photon response from our SPDC biphoton source. If the short-wavelength part of the SPDC spectrum is suppressed, the single-photon response is expected to be very small. In our experiment, this part of the spectrum, along with the UV pump, was suppressed by narrow-band and by low-pass optical filters down to the dark noise of the PMT, which was at the level of a few counts per second. The PMT was moved in and out of the image plane. Although it always collected the same amount of light on its photo cathode which, is 5 mm in diameter, all of the photon pairs are expected to focus to diffraction-limited spots only in the image plane. Therefore, the two-photon photo-electric signal should have a peak in the image plane. We have observed the expected behavior, see Fig.8. However, the origin of this peak turns out not to be due to the predicted two-photon effect, as discussed below.

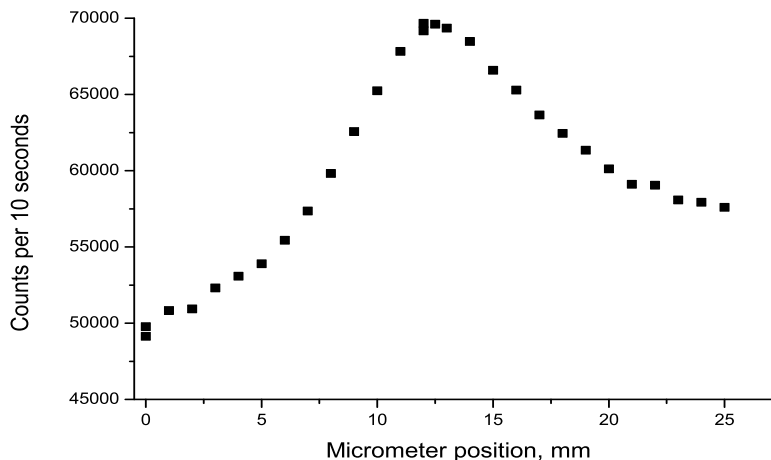


Figure 8: Two-photon PMT response to the biphoton SPDC light as a function of the PMT position in Fig.7.

Repeating the same experiment for attenuated CW laser light, we see a similar peak. Evidently, this peak arises from the fact that, in both the case of SPDC and the ordinary laser, the illuminated spot is the smallest, and therefore the intensity is the highest, in the image plane. Since the total light power is independent of the photo cathode position, we obviously have some kind of a nonlinear (two-photon) process. This process, however, is very slow, which corresponds to a very large longitudinal extent of the two-photon detection volume. Physically, this most likely corresponds to a long lifetime of some intermediate state. As a result, a tight temporal (longitudinal) correlation of the biphoton field gives it no advantage over the attenuated classical light that has photons with Poissonian statistics.

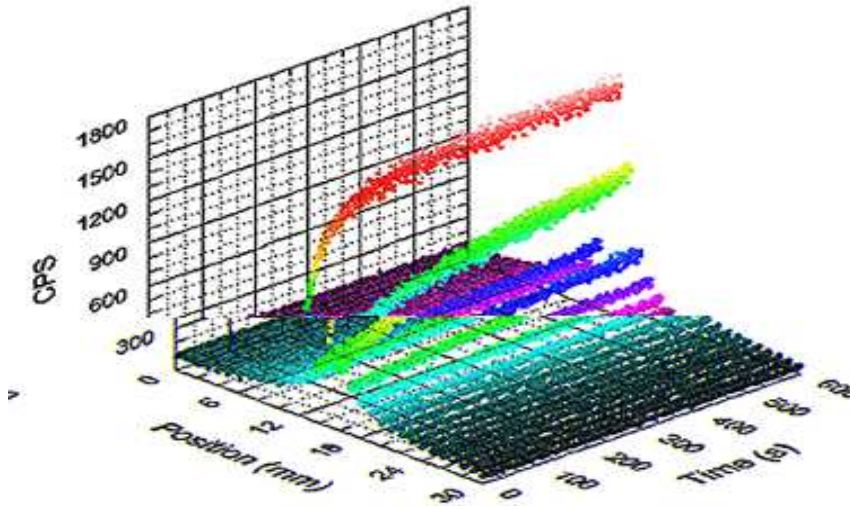


Figure 9: Dependence of the two-photon counting rate (in counts per second) on the photo cathode position with respect to the lens and on time.

Trying to determine the intermediate state lifetime, to characterize our prospective two-photon detector, we found that its two-photon sensitivity itself depends on time. This dependence is stronger for higher light intensities, that is, near the image plane. The situation can be described as the two-photon self-sensitization, which is illustrated in Fig.9 for an attenuated diode laser at around 650 nm. From Fig.9 we can see that the sensitization rate is higher for a higher intensity and that for the maximum light level we used (1.4 nW focused in a spot of $35\text{ }\mu\text{m}$ in diameter) the two-photon sensitivity can be increased by more than an order of magnitude over a period of time of about 100 seconds, at which point it saturates. We have also observed qualitatively similar power-dependent sensitization effect when keeping the illuminated area constant but changing the light power. However the preference was given to the other method because of experimental convenience.

The photo-cathode remains saturated for some time after the light is turned off. Its relaxation back to the initial unsaturated sensitivity, as a function of time, is shown in Fig.10. To obtain this dependence, we have sensitized the photo cathode at the maximum light level, and then let it sit in the dark, while periodically probing its response with weak light pulses. This response has been normalized to the probe light photon flux to yield directly the quantum efficiency. We found that the resulting decay curve fits to a bi-exponential function with decay constants of around 100 and 5 seconds, which may indicate the presence of at least two intermediate states. The fact that optical processes at room temperatures can be so slow is very surprising and suggests that we may be seeing the ion transport processes as opposed to electron ones. Another possible explanation is that the electrons undergo indirect single-photon transition into deep trapped states in the bandgap. The nature of these states is unclear to us at this point. These could be surface states as well as localized impurity states, or the states associated with structural defects.

In support of the deep-state hypothesis, we should mention the experimental observations of the photoconductivity dynamics in GaAs [35]. In this experiment, filling the deep traps by the photo-activated electrons from a valence band results in a life-time increase of the electrons in the conduction band. The activation and relaxation time scales in this process are close to what we observe for Cs_2Te .

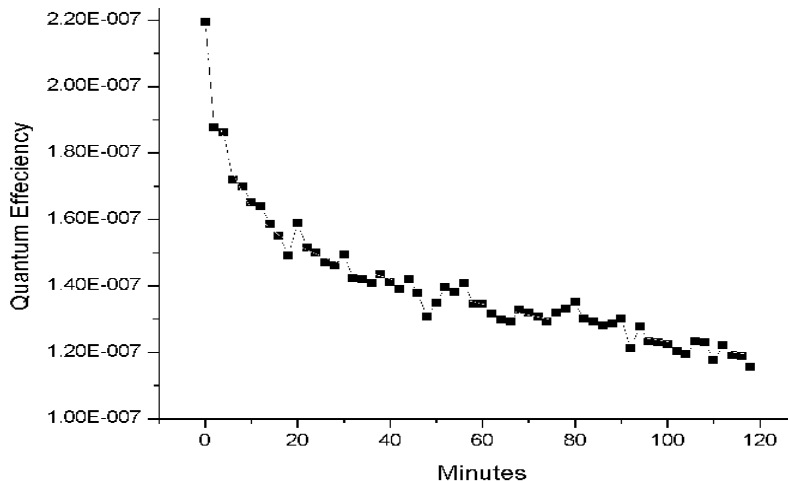


Figure 10: Relaxation curve for a self-sensitized Cs_2Te photo cathode.

5 Conclusions and perspectives

We have considered two types of two-photon processes that can be demonstrated with a faint biphoton field from SPDC and may in principle enable a fast two-photon detector: a process of coherent frequency up-conversion in an optically nonlinear media, and a two-photon photo-electric effect on a semiconductor photo-cathode. This is far from a complete list of processes that can be studied in this context. As the most obvious examples of the two-photon processes left beyond the scope of the present work, we would like to mention the internal photo-electric effect in broad-bandgap semiconductors; ionization of gases and especially of alkali gases [36,37]; and photo-chemical processes such as two-photon fluorescence and polymerization, e.g. [38].

Internal two-photon photo-electric processes should be similar to the external ones with the only difference that for the former the excited photo electrons remain in the conduction band and do not get emitted into vacuum. The internal processes can occur at much further distances from the surface than the external ones. This may simplify description of the internal processes by allowing one to neglect the effects of surface states and surface-bound impurities. We plan on studying this effect and expect that understanding of the mechanisms accompanying the external two-photon photo-electric effect will help.

Two-photon ionization of hydrogen-like gases is an example of a process that could be described analytically. Its simplicity is very attractive for research, however extremely

low detection cross section, resulting from a low concentration of atoms in a gas, presents a serious experimental challenge in the case of a faint biphoton field. In photo-chemical fluorescence processes, on the other hand, the two-photon cross-section of an individual molecule can be quite large (reaching $1,250 \times 10^{-50} \text{ cm}^4 \text{ s}$ per photon [38]), while the concentration of molecules is also much larger than in gases. The two-photon polymerization is a subject of a great interest, since this is the key to the quantum two-photon lithography. While the two-photon polymerization of specially designed photoresists with strong laser pulses has been successfully demonstrated by several groups, e.g. [38–40], the attempts to reproduce the same effect with biphoton field have not so far succeeded. While there are still several questions concerned with the photoresists properties (such as the reciprocity failure for long exposures, the role of thermal mechanisms, etc.) that need to be studied in order to achieve the success, the present study helps to answer one of the key questions by exploring the transverse correlation properties of the biphoton light. Specifically, for any particular imaging system, the transverse correlation function $F(0, \Delta\theta_s, \Delta\theta_i)$ that we have studied can be converted from the angular to linear variables $F(0, \Delta\rho_s, \Delta\rho_i)$ which has a direct relevance for calculating the two-photon exposure doses in quantum lithography.

Acknowledgments

We would like to acknowledge Financial support from the National Aeronautics and Space Administration, the Office of Naval Research, the National Security Agency, the National Reconnaissance Office, and the Advanced Research and Development Activity.

References

- [1] D.N. Klyshko. Transverse photon bunching and two-photon processes in the field of parametrically scattered light. *Sov. Phys. JETP*, **56**:753–59, (1982).
- [2] J.A. Giordmaine and R.C. Miller. Tunable coherent parametric oscillation in LiNbO_3 at optical frequencies. *Phys. Rev. Lett.*, **14**:973–6, (1965).
- [3] A.V. Burlakov, M.V. Chekhova, D.N. Klyshko, S.P. Kulik, A.N. Penin, Y.H. Shih, and D.V. Strekalov. Interference effects in spontaneous two-photon parametric scattering from two macroscopic regions. *Phys. Rev. A*, **56**:3214–25, (1997).
- [4] A.V. Burlakov, M.V. Chekhova, O.A. Karabutova, and S.P. Kulik. Biphoton interference with a multimode pump. *Phys. Rev. A*, **63**:053801, (2001).
- [5] T.B. Pittman, D.V. Strekalov, A. Migdall, M.H. Rubin, A.V. Sergienko, and Y.H. Shih. Can two-photon interference be considered interference of two photons? *Phys. Rev. Lett.*, **77**:1917–20, (1996).
- [6] D.V. Strekalov, T.B. Pittman, and Y.H. Shih. What we can learn about single photons in a two-photon interference experiment. *Phys. Rev. A*, **57**(1):567–570, Jan (1998).

- [7] A. Einstein, B. Podolsky, and N. Rosen. Can quantum mechanical description of reality be considered complete? *Phys. Rev.*, **35**:777–780, (1935).
- [8] Pan JW, Bouwmeester D, Daniell M, Weinfurter H, and Zeilinger A. Experimental test of quantum nonlocality in three-photon greenberger-horne-zeilinger entanglement. *Nature*, **403**:515–519, (2000).
- [9] Bouwmeester D, Pan JW, Mattle K, Eibl M, Weinfurter H, and Zeilinger A. Experimental quantum teleportation. *Nature*, **390**:575–579, (1997).
- [10] Kim YH, Kulik SP, and Shih YH. Quantum teleportation of a polarization state with a complete bell state measurement. *Phys. Rev. Lett.*, **86**(7):1370–1373, Feb (2001).
- [11] A.K. Ekert. Quantum cryptography based on Bell’s theorem. *Phys. Rev. Lett.*, **67**:661–663, (1991).
- [12] Yuen HP. Generation, detection, and application of high-intensity photon-number-eigenstate fields. *Physical Review Letters*, **56**:2176–79, (1986).
- [13] Yurke B, McCall SL, and Klauder JR. SU(2) and SU(1,1) interferometers. *Phys. Rev. A*, **33**:4033–54, (1986).
- [14] L.A. Lugiato, A. Gatti, and E. Brambilla. Quantum imaging. *J. Opt. B*, **4**:S1–S8, (2002).
- [15] R. Jozsa, D.S. Abrams, J. P. Dowling, and C. P. Williams. Quantum clock synchronization based on shared prior entanglement. *Phys. Rev. Lett.*, **85**:2010–13, (2000).
- [16] V. Giovannetti, S. Lloyd, and L. Maccone. Positioning and clock synchronization through entanglement. *Phys. Rev. A*, **65**:022309, (2002).
- [17] A.N. Boto, P. Kok, D.S. Abrams, S.L. Braunstein, C. P. Williams, and J.P. Dowling. Quantum interferometric optical lithography: exploiting entanglement to beat the diffraction limit. *Phys. Rev. Lett.*, **85**:2733–36, (2000).
- [18] P. Kok, A.N. Boto, D.S. Abrams, C. P. Williams, S. L. Braunstein, and J. P. Dowling. Quantum interferometric optical lithography: Towards arbitrary two-dimensional patterns. *Phys. Rev. A*, **63**:063407, (2001).
- [19] Bjork G, Sanchez-Soto LL, and Soderholm J. Entangled-state lithography: Tailoring any pattern with a single state. *Phys. Rev. Lett.*, **86**:4516–19, (2001).
- [20] M. D’Angelo, M.V. Chekhova, and Y.H. Shih. Two-photon diffraction and quantum lithography. *Phys. Rev. Lett.*, **87**:013602, (2001).
- [21] D.V. Strekalov and J.P. Dowling. Two-photon interferometry for high-resolution imaging. *J. of Mod. Opt.*, **49**:519–527, (2002).

- [22] G. Gilbert and M. Hamrick. Practical quantum cryptography: A comprehensive analysis (part one). *quant-ph/0009027*, (2000).
- [23] J. Perina. *Coherence of light*. D. Reidel Publishing Comp., 2nd edition, (1985).
- [24] J. Javanainen and P.L. Gould. Linear intensity dependence of a two-photon transition rate. *Phys. Rev. A*, **41**:5088–91, (1990).
- [25] D.N. Klyshko. *Photons and Non-linear Optics*. Gordon and Breach Science, New York, 1988.
- [26] Y.H. Shih and C.O. Alley. New type of Einstein-Podolsky-Rosen experiment using pairs of light quanta produced by optical parametric down conversion. *Phys. Rev. Lett.*, **61**:2921–2924, (1988).
- [27] C.K. Hong, Z.Y. Ou, and L. Mandel. Measurement of subpicosecond time intervals between two photons by interference. *Phys. Rev. Lett.*, **59**:2044–2046, (1987).
- [28] M.H. Rubin. Transverse correlation in optical spontaneous parametric down conversion. *Phys. Rev. A*, **54**:5349, (1996).
- [29] A.F. Abouraddy, B.E.A. Saleh, A.V. Sergienko, and M.C. Teich. Role of entanglement in two-photon imaging. *Phys. Rev. Lett.*, **87**:123602, (2001).
- [30] M.B. Nasr, A.F. Abouraddy, M.C. Booth, B.E.A. Saleh, A.V. Sergienko, M.C. Teich, M. Kempe, and Ralf Wolleschensky. Biphoton focusing for two-photon excitation. *Phys. Rev. A*, **65**:023816, (2002).
- [31] Y.H. Shih, A.V. Sergienko, M.H. Rubin, T.E. Kiess, and C.O. Alley. Two-photon entanglement in type-II parametric down-conversion. *Phys. Rev. A*, **50**:23–28, (1994).
- [32] C.Rulliere, editor. *Femtosecond Laser Pulses, Principles and Experiments*. Springer-Verlag, (1998).
- [33] T. Hattori, Y. Kawashima, M. Daikoku, H. Inouye, and H. Nakatsuka. Femtosecond two-photon response dynamics of photomultiplier tubes. *Jpn. J. Appl. Phys.*, **39**:4793–98, (2000).
- [34] R. A. Powell, W. E. Spicer, G. B. Fisher, and P. Gregory. Photoemission studies of cesium telluride. *Phys. Rev. B*, **8**:15, (1973).
- [35] B. Santic, U.V. Desnica, N. Radic, D. Desnica, and M. Pavlovic. Photoconductivity transients and photosensitization phenomena in semiinsulating GaAs. *J. of Appl. Phys.*, **73**:5181–84, (1993).
- [36] N. Ph. Georgiades, E. S. Polzik, and H. J. Kimble. Two-photon spectroscopy of the $6s^{1/2}$ to $6d^{5/2}$ transition of trapped atomic cesium. *Optics Letters*, **19**, (1994).

- [37] N. Ph. Georgiades, E. S. Polzik, K. Edamatsu, and H. J. Kimble. Nonclassical excitation for atoms in a squeezed vacuum. *Phys. Rev. Let.*, **19**, (1995).
- [38] B.H. Cumpston *et al.* Two-photon polymerization initiators for three-dimensional optical data storage and microfabrication. *Nature*, **398**:51–54, (1999).
- [39] G.Witzgall, R. Vrijen, E. Yablonovitch, V. Doan, and B.J. Schwartz. Single-shot two-photon exposure of commercial photoresist for production of three-dimensional structures. *Optics Letters*, **23**:1745–47, (1998).
- [40] S. Kawata, H.-B. Sun, T. Tanaka, and K. Takada. Finer features for functional microdevices. *Nature*, **412**:697–98, (2001).